

Generating Probabilistic Safety Guarantees for Neural Network Controllers

Sydney M. Katz · Kyle D. Julian ·
Christopher A. Strong · Mykel J.
Kochenderfer

Received: date / Accepted: date

Abstract Neural networks serve as effective controllers in a variety of complex settings due to their ability to represent expressive policies. The complex nature of neural networks, however, makes their output difficult to verify and predict, which limits their use in safety-critical applications. While simulations provide insight into the performance of neural network controllers, they are not enough to guarantee that the controller will perform safely in all scenarios. To address this problem, recent work has focused on formal methods to verify properties of neural network outputs. For neural network controllers, we can use a dynamics model to determine the output properties that must hold for the controller to operate safely. In this work, we develop a method to use the results from neural network verification tools to provide probabilistic safety guarantees on a neural network controller. We develop an adaptive verification approach to efficiently generate an overapproximation of the neural network policy. Next, we modify the traditional formulation of Markov decision process (MDP) model checking to provide guarantees on the overapproximated policy given a stochastic dynamics model. Finally, we incorporate techniques in state abstraction to reduce overapproximation error during the model checking process. We show that our method is able to generate meaningful probabilistic safety guarantees for aircraft collision avoidance neural networks that are loosely inspired by Airborne Collision Avoidance System X (ACAS X), a family of collision avoidance systems that formulates the problem as a partially observable Markov decision process (POMDP).

Keywords Neural Network Controller · Verification · Model Checking · Safety

S.M. Katz (corresponding author), K.D. Julian, M.J. Kochenderfer
Stanford University, Department of Aeronautics and Astronautics
Stanford, CA, USA
E-mail: {smkatz, kjulian3, mykel}@stanford.edu
ORCID: 0000-0001-8376-5145, 0000-0002-6247-1874, 0000-0002-7238-9663

C.A. Strong
Stanford University, Department of Electrical Engineering
Stanford, CA, USA
E-mail: castrong@stanford.edu
ORCID: 0000-0002-8914-6852

1 Introduction

Neural networks provide a means to represent complex control policies. Because of their ability to represent an expressive policy, they are particularly useful in high-dimensional problems where an agent must make decisions over a large input space (Mnih et al., 2015). Recently, neural networks have been proposed as controllers in safety-critical applications such as aircraft collision avoidance and autonomous driving (Julian et al., 2016, 2019a; Bouton, 2020; Pan et al., 2017).

This work uses aircraft collision avoidance as a running example. Neural networks have been demonstrated as space-efficient controllers for a family of aircraft collision avoidance systems called the Airborne Collision Avoidance System X (ACAS X) (Julian et al., 2016, 2019a). ACAS X formulates the collision avoidance problem as a partially observable Markov decision process (POMDP). The POMDP is solved offline and the solution is loaded onto the aircraft in the form of a large numeric lookup table, which is used to provide optimal advisories during flight (Kochenderfer and Chryssanthacopoulos, 2011; Kochenderfer et al., 2012; Olson, 2015; Owen et al., 2019). Julian et al. (2019a) showed that it is possible to decrease the memory footprint of the lookup table by training a neural network to take its place. The neural network representation decreases the required storage by a factor of 1,000 while maintaining comparable performance to the table representation in simulation.

Despite the substantial benefits, using a neural network in this setting presents new challenges. Due to the inherent complexity and unpredictable nature of neural networks, they are difficult to certify for use in safety-critical applications. Performance in Monte Carlo simulations is not enough to guarantee that the network will provide a safe output in all scenarios. To this end, recent work in formal methods has resulted in algorithms and tools for verifying properties of neural networks (Katz et al., 2017, 2019; Wang et al., 2018; Tjeng et al., 2017). Liu et al. (2019) provide an overview of neural verification methodologies that incorporate techniques from reachability, optimization, and search. Given a bounded input set, these tools provide guarantees on characteristics of the output set.

In the context of aircraft collision avoidance, we can use neural network verification tools to determine all possible collision avoidance maneuvers that a neural network may output for points in a particular input region. This methodology was used to prove properties of neural networks trained on an early prototype of ACAS Xu, the version of ACAS X developed for unmanned aircraft (Katz et al., 2017; Owen et al., 2019). An example property that should hold for the ACAS Xu networks is that the system should always issue an alert if an intruder is directly in front of the ownship. Katz et al. (2017) use the Reluplex algorithm for neural network verification to prove this property, along with a number of other intuitive properties that must hold for safe operation. Other verification tools have proven the same properties as a benchmark (Wang et al., 2018; Liu et al., 2019).

Using neural network verification tools to prove properties in this manner represents a step towards the ability to certify neural networks as safe; however, these works simply test properties that should hold based on intuition. In order to guarantee safety, there is a need for a more principled approach to selecting the properties that a neural network must satisfy for safe operation. By taking into account a dynamic model to create a closed-loop system, we can better understand what constitutes a “safe” neural network output. Julian et al. (2019b)

define “safeable” regions for each action, in which even the worst case trajectory created by following the action will still be safe. This method, however, generates safety constraints that are difficult to satisfy. If the decision boundary of the neural network policy does not line up exactly with the boundary of the “safeable” region, the verification tool will always flag some states as unsafe.

To better approximate the true closed-loop system, previous work has used various forms of reachability analysis (Julian and Kochenderfer, 2019b,a; Huang et al., 2019; Xiang and Johnson, 2018; Xiang et al., 2018, 2019; Dutta et al., 2019; Ivanov et al., 2019). Reachability approaches typically involve combining work in neural verification with existing reachability methods from fields such as ordinary differential equations and hybrid systems. Other approaches involve combining the neural network controller with a neural network representation of the dynamics and performing the neural network verification on the entire closed-loop system (Sidrane and Kochenderfer, 2019; Akintunde et al., 2018).

A limitation of reachability approaches is their deterministic nature. For instance, Julian and Kochenderfer (2019b) applied reachability analysis to generate safety guarantees of networks loosely inspired by ACAS Xu. The analysis works by dividing the state space into small cells, running each cell through a verification tool to determine the possible advisories the network could output, and using the result to determine whether states involving a collision were in the reachable set. While this approach was able to provide deterministic guarantees that the aircraft would not collide, it required strong assumptions on the dynamics of the intruding aircraft for the conclusion to hold (Julian and Kochenderfer, 2019a). As intruder dynamics constraints are relaxed, there exists a set of adversarial intruder accelerations that could result in a collision. Even though the intruder is unlikely to follow this acceleration pattern, the binary nature of the reachability analysis requires collision states to be flagged as reachable.

In this work, instead determining solely whether unsafe states are reachable, we develop a method that uses a stochastic dynamics model to provide probabilistic safety guarantees. Similar to Julian and Kochenderfer (2019b), we divide the input space into small cells and run each input region through a neural network verification tool (Julian and Kochenderfer, 2019a,b). Using the results of the neural verification tool to define an action space, we formulate the model checking problem as a Markov decision process (MDP). This formulation allows us to draw upon techniques from MDP model checking to approximate the probability of reaching an unsafe state from any particular cell given a probabilistic model of the dynamics (Baier and Katoen, 2008; Lahijanian et al., 2011; Bouton et al., 2020; Bouton, 2020).

We modify the model checking formulation to ensure an overapproximation of the probabilities and outline both online and offline methods to reduce overapproximation error. Specifically, we develop an adaptive verification method that addresses limitations mentioned in previous work to efficiently divide the input region into cells (Julian and Kochenderfer, 2019a). We show that this method better approximates the decision boundaries of the neural network and processes the input space faster than a naïve approach to state space discretization. We further reduce overapproximation error by using ideas from state abstraction to split safety-critical regions of the state space during the solving process (Munos and Moore, 2002). We apply our method to aircraft collision avoidance neural net-

works and show that we can use it to provide meaningful safety guarantees on a neural network controller.

2 Problem Formulation

We begin by formulating the verification problem as a Markov decision process (MDP). An MDP is a way of encoding a sequential decision making problem where an agent’s action at each time step depends only on its current state (Kochenderfer, 2015). An MDP is defined by the tuple $(\mathcal{S}, \mathcal{A}, T, R, \gamma)$, where \mathcal{S} is the state space, \mathcal{A} is the action space, $T(s, a, s')$ is the probability of transitioning to state s' given that we are in state s and take action a , $R(s, a)$ is the reward for taking action a in state s , and γ is the discount factor.

Using this formulation, we can solve for a policy $\pi(s)$ that maps states to actions. To do so, we define a value function $Q(s, a)$ that represents the discounted sum of expected future rewards when taking action a from state s . The optimal value function $Q^*(s, a)$ can be found using a form of dynamic programming called value iteration. Value iteration relies on iterative updates to the Bellman equation (Bellman, 1952)

$$Q^*(s, a) = R(s, a) + \gamma \sum_{s' \in \mathcal{S}} T(s, a, s') \max_{a' \in \mathcal{A}} Q^*(s', a') \quad (1)$$

The policy $\pi(s)$ can be defined by simply choosing the action with the maximum value at state s

$$\pi(s) = \arg \max_{a \in \mathcal{A}} Q^*(s, a) \quad (2)$$

We assume that we are given a neural network controller that represents the value function for a policy π , which maps points in a bounded input space \mathcal{S} to an action in the action space \mathcal{A} . Our goal is to guarantee that the controller will provide safe output actions for all points in \mathcal{S} . We break the problem into two steps. The first step involves using a neural verification tool to obtain an overapproximated neural network policy $\tilde{\pi}$. Using this policy, the second step uses probabilistic model checking to generate an overapproximated probability of reaching an unsafe state from each point in \mathcal{S} . For both steps, we develop techniques to reduce overapproximation error in the estimated probabilities.

2.1 Policy Overapproximation

To obtain an overapproximated policy, we divide the input space \mathcal{S} into a set of smaller regions called cells, $c \in \mathcal{C}$. For a given cell c , we use a neural verification tool to obtain the possible actions $\mathcal{A}_c \subseteq \mathcal{A}$ that the neural network could output for some point in c . The results provide a policy $\tilde{\pi}(c)$ that maps a cell c to a subset of the action space \mathcal{A}_c in contrast with $\pi(s)$, which maps a specific state in the input space to a specific action. We assume that any point in c could yield any action in \mathcal{A}_c . Therefore, any cell that has multiple actions in \mathcal{A}_c contributes to an overapproximation of the neural network policy. Policy overapproximation is the first source of overapproximation error in the probability of reaching an unsafe state.

2.2 Probabilistic Model Checking

Probabilistic model checking for MDPs has been well studied and often involves determining the probability of satisfying a property expressed using Linear Temporal Logic (LTL) (Baier and Katoen, 2008; Lahijanian et al., 2011; Bouton et al., 2020). An LTL formula consists of atomic propositions connected by logical or temporal operators (Baier and Katoen, 2008). Our goal is to assign a probability $\Pr^{\tilde{\pi}}(c)$ of satisfying the LTL specification to each cell $c \in \mathcal{C}$. For any LTL formula, this computation reduces to a reachability problem for a set of states \mathcal{B} (Baier and Katoen, 2008; Bouton, 2020). In traditional MDP model checking, we seek to find the maximum probability of reaching states in \mathcal{B} while following policy π for each state $s \in \mathcal{S}$. This probability can be written recursively as

$$\Pr^{\pi}(s) = \sum_{s' \in \mathcal{S}} T(s' | s, \pi(s)) \Pr^{\pi}(s') \quad (3)$$

for all states $s \notin \mathcal{B}$. All states $s \in \mathcal{B}$ are assigned a probability of one.

We can modify this equation to determine the probabilities for each cell $c \in \mathcal{C}$ using our overapproximated neural network policy $\tilde{\pi}$ as

$$\Pr^{\tilde{\pi}}(c) = \max_{a \in \mathcal{A}_c} \sum_{c' \in \mathcal{C}} T(c' | c, a) \Pr^{\tilde{\pi}}(c') \quad (4)$$

where \mathcal{A}_c uses the neural verification results and contains the actions that could be taken in cell c . All cells in \mathcal{B} are assigned a probability of one. Equation (4) can also be written in a form that is analogous to the state-action value function in eq. (1) to represent the probability of satisfying the LTL formula when action a is taken from cell c as follows

$$\Pr^{\tilde{\pi}}(c, a) = \sum_{c' \in \mathcal{C}} T(c' | c, a) \max_{a' \in \mathcal{A}_c} \Pr^{\tilde{\pi}}(c', a') \quad (5)$$

Noting the similarity between eq. (1) and eq. (5), we can solve for the probabilities using value iteration. The problem reduces to solving for the value function of an MDP with a modified reward function to represent probabilities (Bouton et al., 2020; Bouton, 2020). The immediate reward is one for being in a cell in \mathcal{B} and zero for being in any other cell.

The transition model, $T(c' | c, a)$, is modified to determine transitions between cells rather than states and to ensure that the resulting probabilities represent an overapproximation of the true probabilities. We assume that $T(s' | s, a)$ has n nonzero entries corresponding to n possible outcomes from taking action a . For example, in aircraft collision avoidance, this corresponds to the possible accelerations an aircraft may follow when presented with a particular collision avoidance advisory. Let p_i represent the i th nonzero entry in $T(s' | s, a)$. Propagating the upper and lower bounds of a cell c through the dynamics model for each outcome $i \in 1, \dots, n$ yields subregions of the state space $\mathcal{S}_{1:n}$. We define $\mathcal{C}_{1:n}$ as the sets of cells that overlap with $\mathcal{S}_{1:n}$. In order to preserve the overapproximation in our probabilities, we assign all of the probability for outcome i to the worst-case cell in \mathcal{C}_i as follows

$$T(c' | c, a) = \sum_i \begin{cases} p_i, & \text{if } c' = \arg \max_{c'' \in \mathcal{C}_i} \Pr^{\tilde{\pi}}(c'') \\ 0, & \text{otherwise} \end{cases} \quad (6)$$

Equation (6) preserves the overapproximation by assuming that *all* points in a cell transition to the worst-case next state realizable from *any* point in the cell. Figure 1 shows a two-dimensional visual representation of the transition model with three possible outcomes adapted for use with cells. The light shaded regions indicate the bound on the next states for each probabilistic outcome. Cell groupings $\mathcal{C}'_{1:3}$ are labeled as the cells that overlap with the shaded regions, and the darker cells are examples of cells that may be assigned the probability from the corresponding outcome.

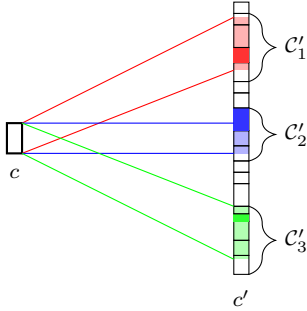


Fig. 1 Two-dimensional illustration of cell transition with three possible outcomes. Each shaded region represents a possible realization of the next state with an associated probability. The dark cells represent the cell that overlaps with the shaded region with the highest probability of satisfying the LTL formula.

3 Reducing Overapproximation Error

The model checking formulation presented here results in two sources of overapproximation error. The first source of error, which we will refer to as policy overapproximation error, is the overapproximation of the policy from the neural verification tools. We assume that the advisories in \mathcal{A}_c may be taken at any point in the cell and that we always take the advisory with the worst-case probability (see the maximization in eq. (5)). Even if the worst-case advisory covers only a small portion of a cell, we must assume that the advisory is possible at any point in the cell.

The second source of error, which we will refer to as worst-case transition error, is the overapproximation in the transition model shown in eq. (6). We assume that all points in the cell transition to the worst-case next cell for a given outcome. In order to produce meaningful probabilistic guarantees, it is crucial that we develop methods to reduce the overapproximation error. In this work, we present both offline and online error reduction methods.

3.1 Offline Reduction: Adaptive Verification

As described in section 2.1, overapproximation error grows with the number of possible advisories in a cell, and cells with only one possible advisory will have no overapproximation error in the policy. Therefore, in order to discretize our space in a way that minimizes policy overapproximation, we seek to minimize the volume of the input space occupied by cells that have multiple possible advisories. Figure 2 shows an example of two possible discretizations of the input space for an example policy. While both discretizations contain the same number of cells, the second discretization has a smaller area of the input space covered by cells with multiple possible actions and therefore a smaller overapproximation error. Our goal is to develop a verification strategy that will automatically generate a discretization similar to the rightmost discretization in fig. 2.

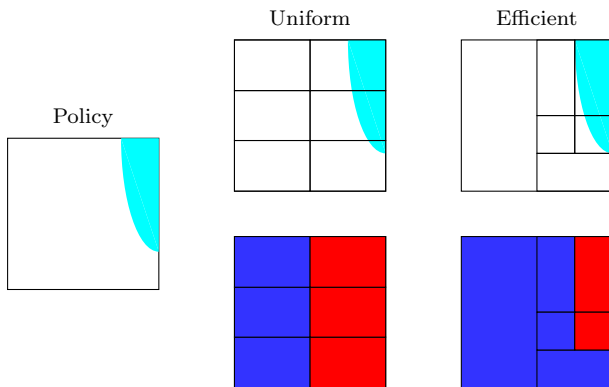


Fig. 2 Two possible discretizations of the input space for the simple policy with two possible actions shown on the left. The white region corresponds to the first action, and the light blue region corresponds to the second action. The top row shows an overlay of the discretization on the policy, while bottom row shows the corresponding number of actions in each cell. Blue cells have one possible action, while red cells have two possible actions.

We use an adaptive verification strategy summarized in algorithm 1 to obtain $\tilde{\pi}$. We begin with a single cell that encompasses all of \mathcal{S} . Each time we evaluate a cell, we run the verification tool to check which advisories are possible in the specified cell to obtain \mathcal{A}_c . If \mathcal{A}_c contains more than one advisory and the cell exceeds the minimum cell size, we split the cell into smaller cells. Splitting continues until all cells are either below the minimum cell width in the splitting dimension or have a single advisory in \mathcal{A}_c .

Because calls to neural verification tools are computationally expensive, we want to select a splitting strategy that will allow us to minimize the number of calls. We tested two splitting strategies. The first splitting strategy, which we will refer to as *all split*, simply splits the cell along all dimensions at the midpoint. The second splitting strategy, which we will refer to as *informed split*, attempts to speed up the verification process by first evaluating the neural network at the corners of the cell. If the corner points evaluate to different actions, we know that

Algorithm 1 Adaptive Verification

```

1: function ADAPTIVEVERIFICATION(neuralNetwork, inputCell, minCellSize)
2:   initialize  $s$  to empty stack
3:   push inputCell onto  $s$ 
4:   while  $s$  is not empty
5:      $c \leftarrow \text{pop}(s)$ 
6:      $\mathcal{A}_c \leftarrow \text{VERIFICATIONTOOL}(\text{neuralNetwork}, c)$ 
7:     if length of  $\mathcal{A}_c > 1$  and size of  $c > \text{minCellSize}$ 
8:       split  $c$  according to splitting strategy
9:       push the resulting cells to  $s$ 
10:  return  $\tilde{\pi}$ 

```

the verification tool would return multiple possible actions. Therefore, we can split the cell without calling it. Furthermore, we can use the evaluations of the corner points to select the dimensions to split. Figure 3 demonstrates the informed split strategy for different corner evaluations. If the adjacent actions are the same across a particular dimension, we do not split along that dimension. For example, the adjacent actions in the first dimension in the leftmost cell of fig. 3 are equal, so we do not split in the first dimension.

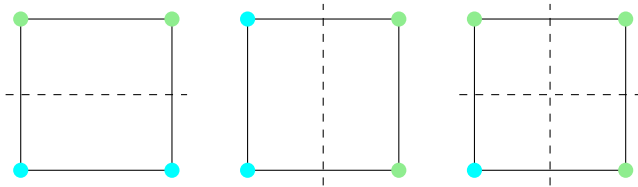


Fig. 3 Example splitting of three cells for the informed splitting strategy based on the actions at the corners. The colored dots represent the actions at the corners with different colors indicating different actions.

3.2 Online Reduction: State Abstraction

While offline error reduction addresses policy overapproximation error, it does not address the second source of error. In order to reduce both types of error, we add online error reduction techniques to the model checking process. The online overapproximation error reduction techniques presented in this work are inspired by state abstraction techniques developed to solve for the value function of MDPs with large state spaces (Munos and Moore, 2002). State abstraction relies on the assumption that large portions of the state space will have low variability in the policy or value function, while other more critical regions of the state space will require a finer resolution for accuracy. Some portions of the state space are safety-critical; however, a large portion of the state space will have a low probability estimate regardless of the action taken. During the solving process, we use heuristics based on our current probability estimate to determine critical portions of the state space. Splitting cells in these critical regions allows us to significantly reduce

overapproximation error during the solving process without making cells in the input space unnecessarily small.

We address the worst-case transition error with an online splitting heuristic based on the maximum range of probability values for next cells. This range is computed as

$$\text{transitionRange} = \max_i \left[\max_{c' \in \mathcal{C}'_i} \Pr^{\tilde{\pi}}(c') - \min_{c' \in \mathcal{C}'_i} \Pr^{\tilde{\pi}}(c') \right] \quad (7)$$

If this range is high, the worst-case transition overapproximation error is likely to be high. Therefore, we split the cell if this range exceeds a specified threshold and the cell is larger than a minimum cell size. The threshold can be tuned by the user to achieve a desired resolution. Splitting the cell will shrink the region of next states for each new cell and reduce the spread of overapproximation error.

The second online splitting heuristic aims to reduce policy overapproximation error and applies to cells that have multiple actions in \mathcal{A}_c . If a cell has multiple actions, we compute the range of the probabilities when taking each action as

$$\text{actionRange} = \max_{a \in \mathcal{A}_c} \Pr^{\tilde{\pi}}(c, a) - \min_{a \in \mathcal{A}_c} \Pr^{\tilde{\pi}}(c, a) \quad (8)$$

If this range exceeds a threshold and the cell is larger than the minimum cell size, we split the cell and rerun the verification on the resulting smaller cells.

3.3 Algorithm Summary

The neural network model checking methods established in this work are summarized in algorithm 2. Inputs to the algorithm include the neural networks to verify, the reachable set encoding the property we wish to verify, an initial cell that covers the entire network input space, the minimum cell size, and the transition and action thresholds. The last three input parameters can be tuned to achieve desired accuracy. A smaller minimum cell size and lower values for the thresholds will result in smaller overapproximation error and therefore a more accurate estimate of the probabilities.

The first step in the algorithm is to obtain an overapproximation of the neural network policy using the adaptive verification method in algorithm 1. Next, the probability is initialized to zero for all cells except those in the reachable set \mathcal{B} , which are initialized to a probability of one. After these preprocessing steps, we begin value iteration with our online splitting heuristics. For each cell, we first compute the transition range according to eq. (7). If the cell satisfies the worst-case transition splitting criterion, we split the cell. Otherwise, we perform the Bellman update (eq. (5)) to compute the probability of collision for taking each action in \mathcal{A}_c from the cell. Using these probabilities and eq. (8), we can compute the action range and decide once again whether to split the cell.

4 Application: Collision Avoidance Neural Networks

We use the aircraft collision avoidance problem as an example application for our methods. The collision avoidance neural networks used in this work are based on

Algorithm 2 Neural Network Model Checking

```

1: function CHECK(neuralNetwork,  $\mathcal{B}$ , inputCell, minCellSize, transitionThreshold, action-
   Threshold)
2:    $\tilde{\pi} \leftarrow$  ADAPTIVEVERIFICATION(neuralNetwork, inputCell, minCellSize)
3:    $\Pr^{\tilde{\pi}}(c) \leftarrow 0$  for all  $c \notin \mathcal{B}$ 
4:    $\Pr^{\tilde{\pi}}(c) \leftarrow 1$  for all  $c \in \mathcal{B}$ 
5:   repeat
6:     initialize  $s$  to an empty stack
7:     push  $c$  onto  $s$  for all  $c \in \mathcal{C}$ 
8:     while  $s$  is not empty
9:        $c \leftarrow$  pop( $s$ )
10:      ranges  $\leftarrow \emptyset$ 
11:      for  $a \in \mathcal{A}_c$ 
12:        compute  $\mathcal{C}'_{1:n}$  from  $c$  for action  $a$ 
13:        add  $\max_i \left[ \max_{c' \in \mathcal{C}'_i} \Pr^{\tilde{\pi}}(c') - \min_{c' \in \mathcal{C}'_i} \Pr^{\tilde{\pi}}(c') \right]$  to ranges
14:        transitionRange  $\leftarrow$  maximum of ranges
15:        if transitionRange > transitionThreshold and size of  $c >$  minCellSize
16:          split  $c$ 
17:          add resulting cells to  $s$ 
18:        else
19:           $\Pr^{\tilde{\pi}}(c, a) \leftarrow \sum_{c' \in \mathcal{C}} T(c' | c, a) \max_{a' \in \mathcal{A}_c} \Pr^{\tilde{\pi}}(c', a')$  for all  $a \in \mathcal{A}_c$ 
20:          actionRange  $\leftarrow \max_{a \in \mathcal{A}_c} \Pr^{\tilde{\pi}}(c, a) - \min_{a \in \mathcal{A}_c} \Pr^{\tilde{\pi}}(c, a)$ 
21:          if actionRange > actionThreshold and size of  $c >$  minCellSize
22:            split  $c$ 
23:            add resulting cells to  $s$ 
24:      until convergence
25:   return  $\Pr^{\tilde{\pi}}$ 

```

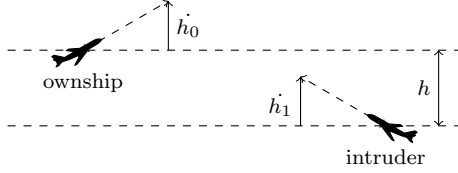
the networks in the VerticalCAS repository developed by Julian and Kochenderfer (2019b). The repository contains an open source collision avoidance logic loosely modeled after the vertical logic used in ACAS X (Julian and Kochenderfer, 2019b). The logic is designed to prevent near mid-air collisions (NMACs), which are defined as a simultaneous loss of separation to less than 500 ft horizontally and 100 ft vertically. To apply model checking to the problem, we must first formulate it as a Markov decision process. We use a similar formulation to what was used to generate the lookup table for ACAS X.

State Space The state space for VerticalCAS consists of five state variables. Table 1 summarizes the variables and their ranges, and fig. 4 provides a visual representation of the state variables. The first three variables summarize the relative positioning and vertical rate of the ownship and intruder aircraft. The next state variable, τ , compactly summarizes the horizontal geometry by representing the time until the horizontal separation between the two aircraft is less than 500 ft. Finally, adding the previous advisory to the state space allows us to penalize a reversal or strengthening of an advisory while still satisfying the Markov property.

Action Space The action space consists of the advisories that the collision avoidance system will provide to the aircraft during flight. The logic has nine possible advisories, which are summarized in table 2. All advisories except COC represent an alert and command the aircraft to a particular vertical rate range. The COC

Table 1 VerticalCAS state variables

Variable	Description	Units	Range (low:high)
h	relative altitude of intruder	ft	-8000 : 8000
\dot{h}_0	ownship vertical rate	ft/s	-100 : 100
\dot{h}_1	intruder vertical rate	ft/s	-100 : 100
τ	time to loss of lateral separation	s	0:40
a_{prev}	previous advisory	N/A	N/A

**Fig. 4** Visual representation of VerticalCAS state variables.

advisory indicates that there is currently no threat of collision with an intruding aircraft.

Table 2 VerticalCAS action space

Action	Description
COC	clear of conflict
DNC	do not climb
DND	do not descend
DES1500	descend ≥ 1500 ft/min
CL1500	climb ≥ 1500 ft/min
SDES1500	strengthen descent to ≥ 1500 ft/min
SCL1500	strengthen climb to ≥ 1500 ft/min
SDES2500	strengthen descent to ≥ 2500 ft/min
SCL2500	strengthen climb to ≥ 2500 ft/min

Transition Model The transition model uses the following linear dynamics model

$$\begin{aligned}
 h &\leftarrow h + \dot{h}_1 + 0.5\ddot{h}_1 - \dot{h}_0 - 0.5\ddot{h}_0 \\
 \dot{h}_0 &\leftarrow \dot{h}_0 + \ddot{h}_0 \\
 \dot{h}_1 &\leftarrow \dot{h}_1 + \ddot{h}_1 \\
 \tau &\leftarrow \tau - 1 \\
 a_{\text{prev}} &\leftarrow a
 \end{aligned} \tag{9}$$

We assume a one second time step corresponding to the 1 Hz update frequency of the collision avoidance system. The dynamics model is made stochastic by assuming distributions over the accelerations of the ownship and intruder. The intruder is assumed to have an equal chance of following accelerations $-g/8$, $g/8$, and 0 ft/s². The ownship follows accelerations \ddot{h}_{1-3} based on its previous advisory with

associated probabilities $p_{1:3}$ shown in table 3. This transition model contains two features that add robustness. First, the ownship is assumed to follow the accelerations associated with its previous advisory (rather than its current advisory), which represents a short delay in the aircraft’s response to the advisory. Additionally, the ownship is assumed to accelerate in the opposite direction of its advisory 20% of the time to further incorporate errors in aircraft response. The probabilistic safety guarantees presented in this paper are based on this stochastic dynamics model.

Table 3 Transition accelerations

Previous Action	Probabilities (p_{1-3})	Accelerations (\ddot{h}_{1-3})
COC	[0.34, 0.33, 0.33]	[0.0, $-g/3$, $g/3$]
DNC	[0.50, 0.30, 0.20]	[$-g/3$, $-g/2$, $g/3$]
DND	[0.50, 0.30, 0.20]	[$g/3$, $g/2$, $-g/3$]
DES1500	[0.50, 0.30, 0.20]	[$-g/3$, $-g/2$, $g/3$]
CL1500	[0.50, 0.30, 0.20]	[$g/3$, $g/2$, $-g/3$]
SDES1500	[0.50, 0.30, 0.20]	[$-g/2.5$, $-g/2$, $g/3$]
SCL1500	[0.50, 0.30, 0.20]	[$g/2.5$, $g/2$, $-g/3$]
SDES2500	[0.50, 0.30, 0.20]	[$-g/2.5$, $-g/2$, $g/3$]
SCL2500	[0.50, 0.30, 0.20]	[$g/2.5$, $g/2$, $-g/3$]

The reward model balances between safety and efficiency with a high penalty for an NMAC and relatively smaller penalties for alerting advisories. Using this formulation, we can solve for the optimal policy using value iteration. Traditionally, the final state-action values result in a large numeric lookup table. To reduce the on-board memory requirements, Julian et al. (2019a) train a neural network representation to approximate the state-action value function. One network is trained for each discrete previous advisory. The values of the other four state variables in table 1 make up the four-dimensional input to the network, and the approximate value of each action makes up the nine-dimensional output. Each network has five hidden layers with 25 units each that use rectified linear unit (ReLU) activation functions.

Figure 5 shows a comparison of the neural network policy and lookup table policy for a slice of the state space. The neural network policy closely approximates the table policy with a few subtle differences that are visible in the plot. Even though the alerting regions in the neural network policy appear continuous, the plot is generated by evaluating a finite number of points in the state space and does not guarantee this property. For example, while the region highlighted on the neural network policy in fig. 5 appears to evaluate to CL1500 at all points within it, we cannot guarantee this property just by examining the plotted points. To provide a guarantee that all advisories in that region are in fact CL1500, we use a neural verification tool to obtain \mathcal{A}_c . For this application, we use the Reluval algorithm to verify each cell due to its fast performance on the collision avoidance networks (Liu et al., 2019; Wang et al., 2018).

We can craft an LTL formula to determine the probability of an NMAC by using the temporal operator “eventually,” written as F. Let the atomic proposition N represent whether or not a cell belongs to the NMAC region ($\tau = 0$ seconds and $h < 100$ ft). The LTL formula of interest is FN , read as “eventually N.”

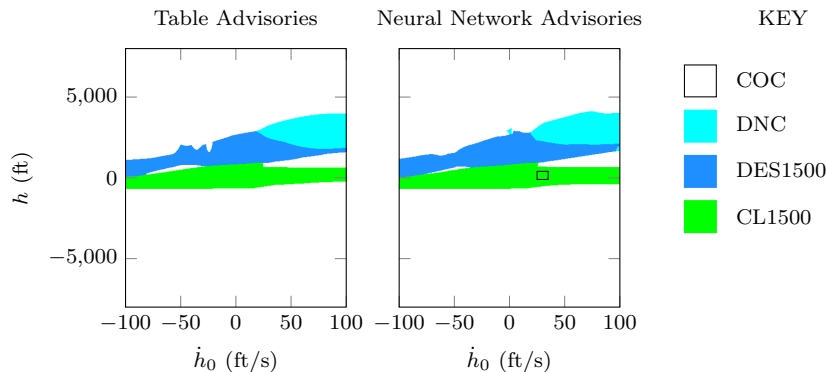


Fig. 5 Comparison of table policy to neural network policy for a slice of the state space. The intruder vertical rate is fixed at -90 ft/s, τ is fixed at 5 seconds, and the previous advisory is COC.

The probability of satisfying this formula corresponds to the probability that a state will eventually reach an NMAC state. This problem is easily converted to a reachability problem. Let \mathcal{N} represent the collection of all cells that satisfy N . We seek to find the maximum probability of reaching cells in \mathcal{N} while following the overapproximated neural network policy.

5 Results

For ease of computation and visualization, we tested our methods on a two-dimensional version of the collision avoidance problem in which the intruder vertical rate is fixed at -90 ft/s before testing on the full scale model. By taking this approach, we were able to better understand the effects of each aspect of the algorithm. Therefore, the results summarizing the effects of the overapproximation reduction techniques were generated using the two-dimensional model. After providing intuition with these results, we present the results of the full scale model.

5.1 Adaptive Verification

We tested both the all split and informed split adaptive verification splitting strategies to obtain the overapproximated policy $\hat{\pi}$. Figure 6 shows the results of both splitting strategies when the intruder vertical rate is fixed at -90 ft/s, and table 4 shows a comparison of runtime for both the two-dimensional and full scale model for each strategy. We also include the runtime of a uniform, non-adaptive splitting strategy in which all cells are the minimum cell size used in the adaptive strategies. For the full-scale model, the non-adaptive runtime was estimated based on the time required to verify a single cell of the minimum cell size. Time trials were run on a single 4.20 GHz Intel Core i7 processor. Both adaptive splitting strategies result in small cells around the decision boundaries of the network; however, the informed splitting strategy results in fewer cells.

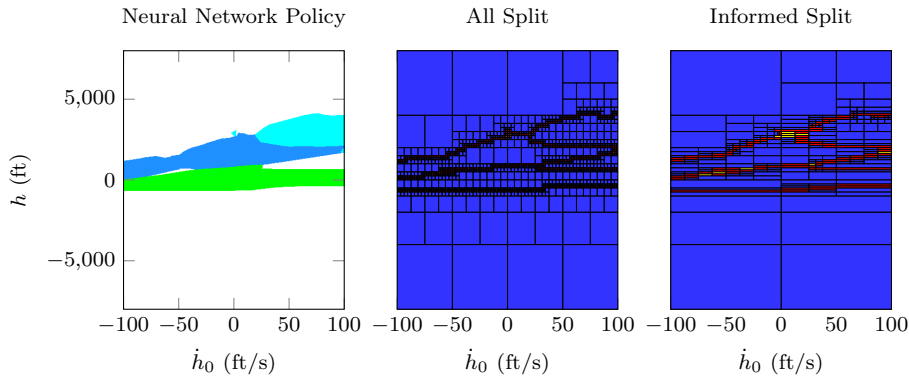


Fig. 6 Comparison of the resulting state space discretization for the adaptive splitting strategies. The intruder vertical rate is fixed at -90 ft/s, τ is 5 seconds, and the previous advisory is COC. Cells that are colored blue have only one possible advisory in \mathcal{A}_c , red cells have two possible advisories, and yellow cells have three or more possible advisories.

Table 4 Adaptive verification timing results

Splitting Strategy	\dot{h}_1	Fixed Time (s)	Full Scale Time (s)
Uniform		235.5	16,000 (est.)
All Split		21.9	2,500.3
Informed Split		5.5	655.6

The adaptive strategies require fewer calls to the verification tool and therefore perform faster than a non-adaptive strategy. Additionally, whenever a cell is split and the resulting cells are reverified, the verification tool only needs to check for the actions that were possible in the larger cell. Informed split is faster than all split because it makes even fewer Reluval calls. Checking the corners to inform the split prevents unnecessary calls and results in fewer cells in the final discretization. Due to its speed, the informed split strategy was selected for the rest of the analysis in this work.

While the adaptive verification technique presented here addresses policy overapproximation error for model checking, it may also be used on its own to analyze neural network policies and detect decision boundaries. The algorithm is an any-time algorithm, and the resolution can be controlled using the minimum cell size parameter. Figure 7 shows results as the parameter is decreased. As the minimum cell size decreases, overapproximation error in the policy also decreases.

After obtaining the overapproximated network policy using adaptive verification, we can run model checking on the cells. Figure 8 shows the results for a slice of the state space. Assuming that an encounter gets initiated with 40 seconds until loss of horizontal separation, a safe policy should have a low probability of NMAC for all states at $\tau = 40$ seconds; however, the probability values at $\tau = 40$ seconds after model checking are close to one, and we therefore cannot provide a safety guarantee with this adaptive verification method alone. We need to introduce the online error reduction techniques.

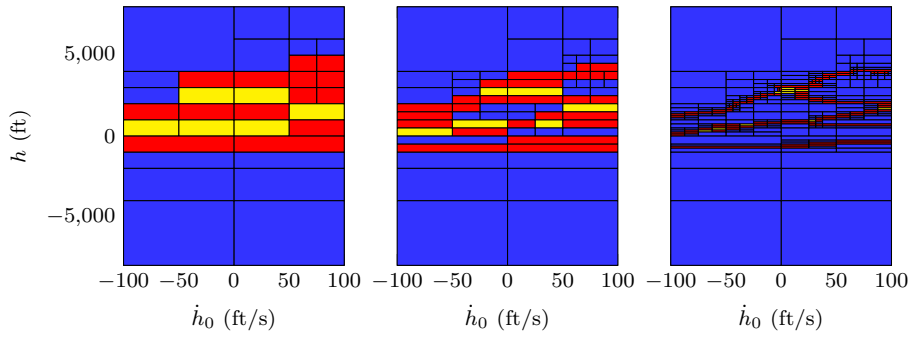


Fig. 7 Adaptive verification results using informed split for decreasing minimum cell sizes (left to right). The intruder vertical rate is fixed at -90 ft/s, τ is 5 seconds, and the previous advisory is COC. Cells that are colored blue have only one possible advisory in \mathcal{A}_c , red cells have two possible advisories, and yellow cells have three or more possible advisories.

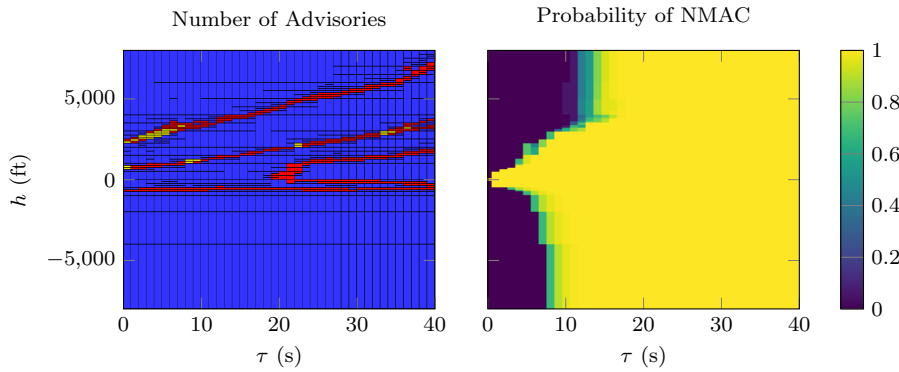


Fig. 8 State space discretization (same color scheme as fig. 6) and overapproximated probability of NMAC with no online overapproximation reduction. The intruder vertical rate is fixed at -90 ft/s, the ownship vertical rate is 0 ft/s, and the previous advisory is COC.

5.2 Online Reduction

Figure 9 displays the model checking results with the online worst-case transition splitting heuristic for the same slice of the state space shown in fig. 8. The algorithm splits cells in a densely packed band along the safety-critical region of the state space where a collision is imminent. The intruder is rapidly descending at 90 ft/s, so the region directly above the ownship is most dangerous. Outside of this band, the state space discretization remains untouched, indicating that the online splitting heuristic only splits states that require a finer resolution.

The overapproximation error in fig. 9 is much lower than the error in fig. 8, and we can now obtain meaningful information from the estimated probabilities. For example, the probabilities are highest at low values of τ when the intruder is above the ownship. The high intruder descent rate results in the upward sloping band of high probability extending away from the NMAC region at $\tau = 0$. At

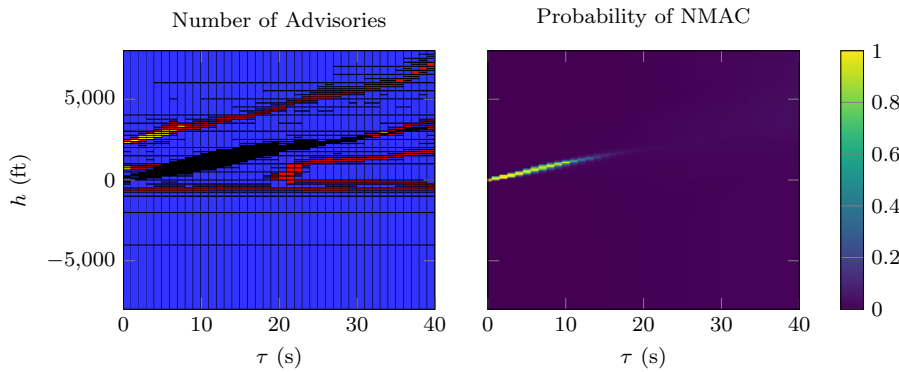


Fig. 9 State space discretization (same color scheme as fig. 6) and overapproximated probability of NMAC with the worst-case transition splitting heuristic. The intruder vertical rate is fixed at -90 ft/s, the ownship vertical rate is 0 ft/s, and the previous advisory is COC.

$\tau = 40$ seconds, the probabilities of collision are significantly lower with a maximum probability of 0.0305 among all cells. The splitting threshold can be tuned to achieve a desired resolution as shown in fig. 10. The highest threshold only splits cells in the extremely safety-critical region near $\tau = 0$. As the threshold is decreased, the band of tightly packed cells extends further away from $\tau = 0$ and overapproximation error decreases.

Figure 11 shows the results when the policy overapproximation heuristic is used in addition to the worst-case transition heuristic. Beyond the splits due to the worst-case transition heuristic, this heuristic results in splits in overapproximated regions at higher values of τ . There is no significant difference in the visualization of probabilities between fig. 9 and fig. 11, and the maximum probability of NMAC at $\tau = 40$ seconds drops from 0.0305 to 0.0268 . The addition of this splitting heuristic did not add a significant benefit over the worst-case transition heuristic, possibly due to the fact that adaptive verification already addresses policy overapproximation error.

Table 5 summarizes the effect of each overapproximation error reduction technique on the maximum overapproximated probability of NMAC for cells at $\tau = 40$ seconds. The adaptive verification technique alone is not enough to reduce overapproximation error to obtain a meaningful estimate of the probability of NMAC. Adaptive verification addresses only policy overapproximation error but does nothing to reduce worst-case transition error. When we add the online splitting heuristic to address worst-case transition error and decrease the splitting threshold, the probability estimate decreases to a more meaningful result. We can guarantee that the probability of NMAC is less than 0.0305 . Adding the online splitting heuristic to further reduce policy overapproximation in key areas of the state space does not have as much of an effect. Nevertheless, it changes the guarantee to a 0.0268 probability of NMAC.

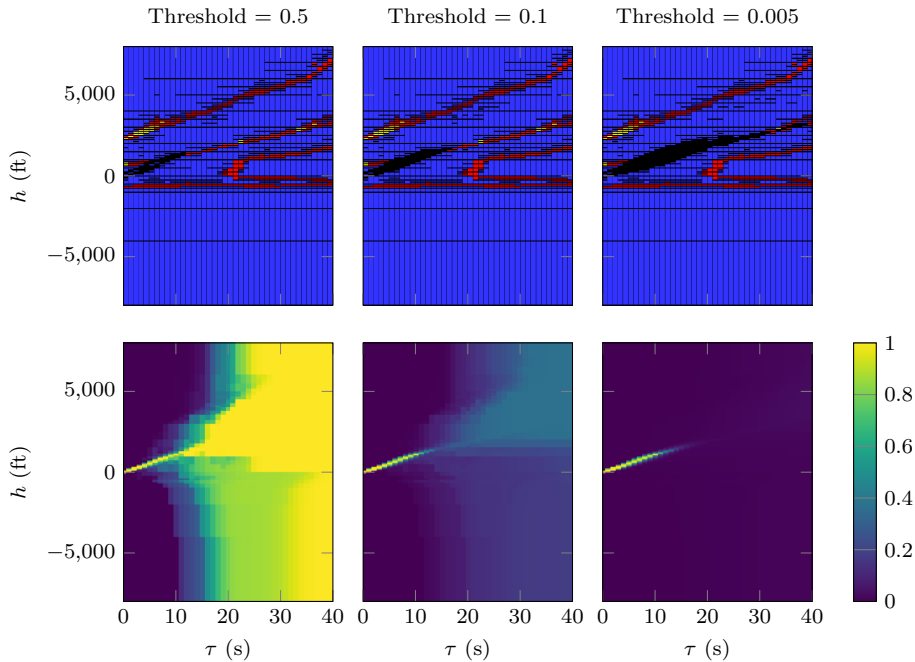


Fig. 10 State space discretization (same color scheme as fig. 6) and overapproximated probability of NMAC using various thresholds for the worst-case transition splitting heuristic. The intruder vertical rate is fixed at -90 ft/s, the ownship vertical rate is 0 ft/s, and the previous advisory is COC.

Table 5 Effect of error reduction methods on overapproximated probability of NMAC

Error Reduction	Transition Threshold	Action Threshold	Probability
Adaptive verification only	-	-	1.0
Worst-case transition	0.5	-	1.0
Worst-case transition	0.1	-	0.372
Worst-case transition	0.005	-	0.0305
All techniques	0.005	0.005	0.0268

5.3 Full Scale Model

After gaining intuition using the two-dimensional model, we applied our method to determine the maximum probability of collision on the full scale model. For computational reasons, the action range threshold was slowly increased throughout the solving process. To analyze the quality of our probability estimates, we generate two baseline probability comparisons. The first comparison is the estimated probability of NMAC when using the large numeric lookup table that the neural network is meant to approximate. This probability is calculated by performing traditional MDP model checking on the table policy and is not guaranteed to be an overapproximation. We also compare with the probability of NMAC detected through 1,000 Monte Carlo simulations from various points in the state

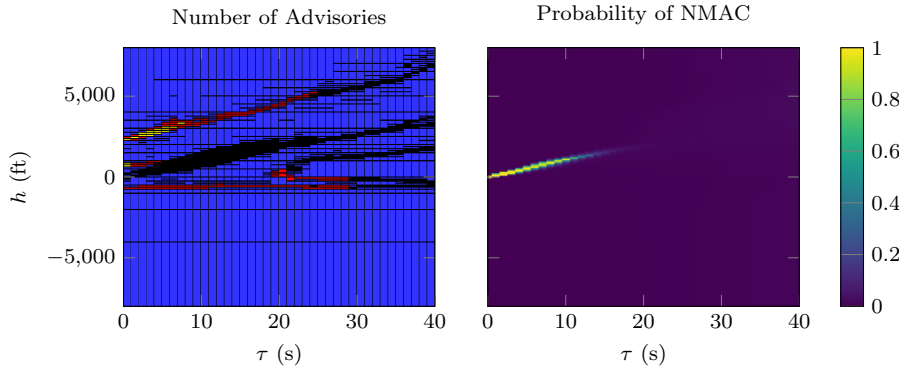


Fig. 11 State space discretization (same color scheme as fig. 6) and overapproximated probability of NMAC with both the worst-case transition splitting heuristic and the policy overapproximation splitting heuristic. The intruder vertical rate is fixed at -90 ft/s, the ownship vertical rate is 0 ft/s, and the previous advisory is COC.

space. While Monte Carlo simulations cannot provide any formal guarantees, they provide a good approximation to the probability of NMAC.

The results for one slice of the state space are shown in fig. 12. All three plots show similar trends. The model checking outputs for the table and neural network are similar with slightly higher probabilities for the neural network. The probabilities are also similar to the Monte Carlo probabilities with the same cells showing high probability of collision; however, the region of high probability is slightly larger in the model checking results. It is clear that the model checking probabilities represent an overapproximation.

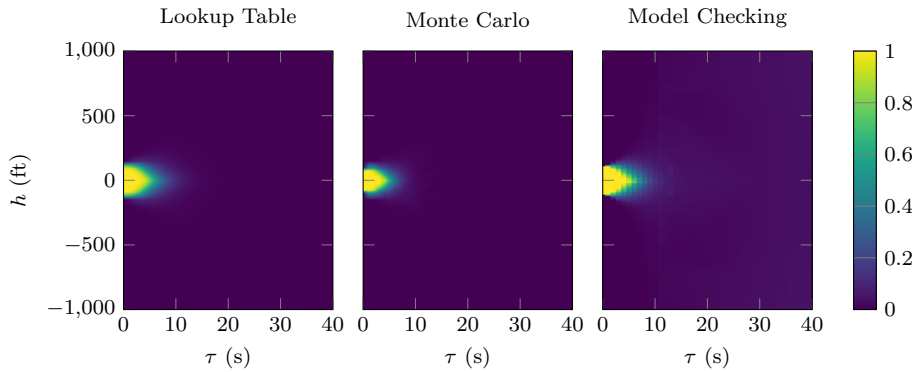


Fig. 12 Comparison of lookup table probabilities of NMAC estimated using traditional MDP model checking, neural network probabilities of NMAC estimated using Monte Carlo simulations, and overapproximated neural network probabilities of NMAC using the model checking formulation in this work. The ownship and intruder vertical rates are both 0 ft/s, and the previous advisory is COC.

Figure 13 shows the maximum probability of collision among all cells as τ is increased for the same slice of the state space shown in fig. 12. At $\tau = 0$ seconds, the maximum probability of NMAC is one, corresponding to cells in the NMAC region. As τ increases for each method, there is a sharp dropoff in probability of NMAC. The overapproximated model checking probabilities are greater than or equal to both the lookup table and Monte Carlo probabilities at all points. The curve, however, remains close to the other curves and represents a tight overapproximation. Furthermore, unlike the Monte Carlo estimate and lookup table model checking estimate, the neural network model checking estimate represents a guarantee on the performance of the neural network policy. The final model checking probability is 0.0473 at $\tau = 40$ seconds. Therefore, with respect to the stochastic dynamics model in section 4, we can guarantee that the probability of NMAC is less than 0.0473 when the intruder and ownship are in level flight.

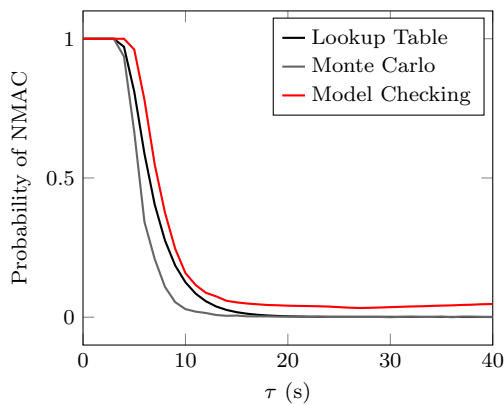


Fig. 13 Probability of NMAC when previous advisory is COC as time to loss of separation increases. The ownship and intruder vertical rates are fixed at 0 ft/s.

We also examined the probability of NMAC when the aircraft are climbing or descending. Figure 14 contains the results when the ownship is climbing at 60 ft/s in comparison to the table and Monte Carlo results, fig. 15 shows the vertical rates when both aircraft are climbing at a rate of 60 ft/s. The trends in the probabilities match the trends seen in the lookup table and Monte Carlo results. In fig. 14, the region of high probability of NMAC extends above the ownship because it starts in a climb.

When both aircraft are climbing at the same rate in fig. 15, the two aircraft are on a direct collision path when they are co-altitude. For this reason, probabilities are high in this region when τ is small. As the time to collision increases, the region shifts downward slightly since the intruder is not executing collision avoidance maneuvers and is therefore most dangerous at altitudes below the ownship. The overapproximated probabilities are again higher than the Monte Carlo probabilities, but the maximum probability of NMAC with these starting states decreases slightly to 0.0462 and 0.0437, respectively.

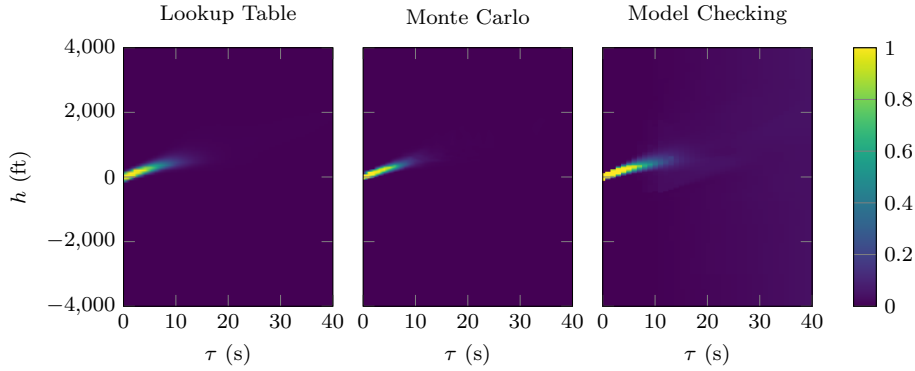


Fig. 14 Comparison of lookup table probabilities of NMAC estimated using traditional MDP model checking, neural network probabilities of NMAC estimated using Monte Carlo simulations, and overapproximated neural network probabilities of NMAC using the model checking formulation in this work. The ownship vertical rate is 60 ft/s, the intruder vertical rate is 0 ft/s, and the previous advisory is COC.

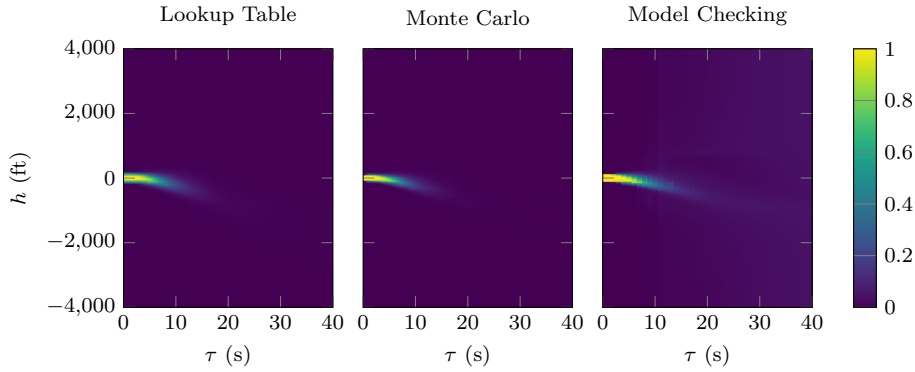


Fig. 15 Comparison of lookup table probabilities of NMAC estimated using traditional MDP model checking, neural network probabilities of NMAC estimated using Monte Carlo simulations, and overapproximated neural network probabilities of NMAC using the model checking formulation in this work. The ownship and intruder vertical rates are both 60 ft/s, and the previous advisory is COC.

The maximum probability of NMAC among all states at $\tau = 40$ is 0.0605 and occurs in the cell in which the intruder is descending at a vertical rate between 77.34 and 78.13 ft/s and is located between 656.25 and 664.06 ft below the ownship. The ownship is also descending rapidly between 99.22 and 100.0 ft/s. Therefore, we can guarantee that the probability of NMAC with respect to the dynamics model outlined in this work when following the neural network policy is less than 0.0605. Tuning parameters such as the online splitting thresholds and minimum cell size allowed us to tighten our bound on the probability. With more computational resources, it is likely that this bound can be tightened further.

6 Conclusion

In this work, we have introduced an approach to generate probabilistic safety guarantees on a neural network controller and applied it to an open source collision avoidance system inspired by the ACAS X neural networks. We demonstrated how techniques in MDP model checking could be applied to verify an overapproximated neural network policy obtained using a neural verification tool. We identified the major sources of overapproximation error in the model checking process and developed both offline and online error reduction techniques to address them.

Our adaptive verification technique efficiently discretizes the input space to obtain an overapproximated neural network policy that minimizes overapproximation error. This method can be used outside of the context of model checking to analyze neural network policies and detect decision boundaries. By combining the adaptive verification results with online splitting heuristics inspired by MDP state abstraction, we are able to provide meaningful probabilistic safety guarantees that follow trends shown in both Monte Carlo analysis and model checking analysis performed on the lookup table that the neural network approximates.

The probabilistic dynamics model used in this work represents a conservative aircraft response model. In the future, other aircraft response models will be analyzed to determine the effect of the model selection on the probabilities. Furthermore, the results can be used to determine unsafe areas of the state space where the neural network policy may need adjustments. For example, at the outset of this work, the model checking method was able to easily detect a bounds error in the neural network policy generation that may have been otherwise easy to overlook. Although we used the method to determine the probability of an NMAC in this work, the general formulation allows us to determine the probability of satisfying any LTL specification. Future work will explore both generating guarantees on other aspects of the aircraft collision avoidance problem as well as for other safety-critical applications such as autonomous driving. The methodology presented here represents a step toward the ability to verify the performance of neural network controllers for use in safety-critical environments.

Declarations

Funding: This research was supported by National Science Foundation Graduate Research Fellowship under Grant No. DGE-1656518. Any opinion, findings, and conclusions or recommendations expressed in this material are those of the authors and do not necessarily reflect the views of the National Science Foundation.

Conflicts of interest/Competing interests: The authors have no conflicts of interest to declare that are relevant to the content of this article.

Availability of data and material: The neural networks used in this research can be found in the “networks” folder of the repository located at <https://github.com/sisl/AdaptiveVerification>.

Code availability: The code for the adaptive verification portion of the work can be found at <https://github.com/sisl/AdaptiveVerification>, and the code for

the model checking is located at <https://github.com/sisl/NeuralModelChecking>. The repository used to generate the networks used in this work is at <https://github.com/sisl/VerticalCAS>.

Conflict of interest

The authors declare that they have no conflict of interest.

References

- Akintunde M, Lomuscio A, Maganti L, Pirovano E (2018) Reachability analysis for neural agent-environment systems. In: International Conference on Principles of Knowledge Representation and Reasoning, pp 184–193
- Baier C, Katoen JP (2008) Principles of model checking. MIT Press
- Bellman R (1952) On the theory of dynamic programming. Proceedings of the National Academy of Sciences of the United States of America 38(8):716
- Bouton M (2020) Safe and scalable planning under uncertainty for autonomous driving. PhD thesis, Stanford University, URL <https://purl.stanford.edu/dy440kv7606>
- Bouton M, Tumova J, Kochenderfer MJ (2020) Point-based methods for model checking in partially observable Markov decision processes. In: AAAI Conference on Artificial Intelligence (AAAI), URL <https://aaai.org/Papers/AAAI/2020GB/AAAI-BoutonM.9314.pdf>
- Dutta S, Chen X, Sankaranarayanan S (2019) Reachability analysis for neural feedback systems using regressive polynomial rule inference. In: Proceedings of the 22nd ACM International Conference on Hybrid Systems: Computation and Control, pp 157–168
- Huang C, Fan J, Li W, Chen X, Zhu Q (2019) ReachNN: Reachability analysis of neural-network controlled systems. ACM Transactions on Embedded Computing Systems (TECS) 18(5s):1–22
- Ivanov R, Weimer J, Alur R, Pappas GJ, Lee I (2019) Verisig: verifying safety properties of hybrid systems with neural network controllers. In: ACM International Conference on Hybrid Systems: Computation and Control, pp 169–178
- Julian KD, Kochenderfer MJ (2019a) Guaranteeing safety for neural network-based aircraft collision avoidance systems. In: Digital Avionics Systems Conference (DASC), DOI 10.1109/DASC43569.2019.9081748, URL <https://arxiv.org/abs/1912.07084>
- Julian KD, Kochenderfer MJ (2019b) A reachability method for verifying dynamical systems with deep neural network controllers (1903.00520), URL <https://arxiv.org/abs/1903.00520>
- Julian KD, Lopez J, Brush JS, Owen MP, Kochenderfer MJ (2016) Policy compression for aircraft collision avoidance systems. In: Digital Avionics Systems Conference (DASC), DOI 10.1109/DASC.2016.7778091
- Julian KD, Kochenderfer MJ, Owen MP (2019a) Deep neural network compression for aircraft collision avoidance systems. AIAA Journal of Guidance, Control, and Dynamics 42(3):598–608, DOI 10.2514/1.G003724, URL <https://arxiv.org/abs/1810.04240>

- Julian KD, Sharma S, Jeannin JB, Kochenderfer MJ (2019b) Verifying aircraft collision avoidance neural networks through linear approximations of safe regions. In: AIAA Spring Symposium, URL <https://arxiv.org/abs/1903.00762>
- Katz G, Barrett C, Dill DL, Julian KD, Kochenderfer MJ (2017) Reluplex: An efficient SMT solver for verifying deep neural networks. In: International Conference on Computer-Aided Verification, URL <https://arxiv.org/abs/1702.01135>
- Katz G, Huang DA, Ibeling D, Julian KD, Lazarus C, Lim R, Shah P, Thakoor S, Wu H, Zeljić A, et al. (2019) The marabou framework for verification and analysis of deep neural networks. In: International Conference on Computer Aided Verification, Springer, pp 443–452
- Kochenderfer MJ (2015) Decision Making Under Uncertainty: Theory and Application. MIT Press
- Kochenderfer MJ, Chryssanthacopoulos J (2011) Robust airborne collision avoidance through dynamic programming. Massachusetts Institute of Technology, Lincoln Laboratory, Project Report ATC-371
- Kochenderfer MJ, Holland JE, Chryssanthacopoulos JP (2012) Next-generation airborne collision avoidance system. Tech. rep., Massachusetts Institute of Technology-Lincoln Laboratory Lexington United States
- Lahijanian M, Andersson S, Belta C (2011) Control of Markov decision processes from PCTL specifications. In: American Control Conference, IEEE, pp 311–316
- Liu C, Arnon T, Lazarus C, Barrett C, Kochenderfer MJ (2019) Algorithms for verifying deep neural networks. arXiv preprint arXiv:190306758
- Mnih V, Kavukcuoglu K, Silver D, Rusu AA, Veness J, Bellemare MG, Graves A, Riedmiller M, Fidjeland AK, Ostrovski G, et al. (2015) Human-level control through deep reinforcement learning. *Nature* 518(7540):529–533
- Munos R, Moore A (2002) Variable resolution discretization in optimal control. *Machine Learning* 49(2-3):291–323
- Olson WA (2015) Airborne collision avoidance system X. Tech. rep., Massachusetts Institute of Technology-Lincoln Laboratory Lexington United States
- Owen MP, Panken A, Moss R, Alvarez L, Leeper C (2019) ACAS Xu: Integrated collision avoidance and detect and avoid capability for UAS. In: IEEE/AIAA Digital Avionics Systems Conference (DASC), pp 1–10
- Pan Y, Cheng CA, Saigol K, Lee K, Yan X, Theodorou E, Boots B (2017) Agile autonomous driving using end-to-end deep imitation learning. arXiv preprint arXiv:170907174
- Sidrane C, Kochenderfer MJ (2019) OVERT: Verification of nonlinear dynamical systems with neural network controllers via overapproximation. In: Workshop on Safe Machine Learning, International Conference on Learning Representations
- Tjeng V, Xiao K, Tedrake R (2017) Evaluating robustness of neural networks with mixed integer programming. arXiv preprint arXiv:171107356
- Wang S, Pei K, Whitehouse J, Yang J, Jana S (2018) Formal security analysis of neural networks using symbolic intervals. In: USENIX Security Symposium, pp 1599–1614, URL <https://www.usenix.org/conference/usenixsecurity18/presentation/wang-shiqi>
- Xiang W, Johnson TT (2018) Reachability analysis and safety verification for neural network control systems. arXiv preprint arXiv:180509944
- Xiang W, Tran HD, Rosenfeld JA, Johnson TT (2018) Reachable set estimation and safety verification for piecewise linear systems with neural network controllers. In: American Control Conference, pp 1574–1579

Xiang W, Lopez DM, Musau P, Johnson TT (2019) Reachable set estimation and verification for neural network models of nonlinear dynamic systems. In: *Safe, Autonomous and Intelligent Vehicles*, Springer, pp 123–144